ponents of frequencies ω_1, ω_2, $2\omega_1$, etc. From Eqs. (1) and (3), we obtain the various velocity components

$$V(\omega_1)=-eE_1\tau_0/m(1+i\omega_1\tau_0), \quad (5)$$

$$V(\omega_2)=-eE_2\tau_0/m(1+i\omega_2\tau_0), \quad (6)$$

and

$$V(2\omega_1-\omega_2)=(n/2\tau_0^2kT)[i(2\omega_1-\omega_2)\tau_0+1]^{-1} \times[mV^2(\omega_1)V^*(\omega_2)+V(\omega_1)kT_e(\omega_1-\omega_2) +V^*(\omega_2)kT_e(2\omega_1)]. \quad (7)$$

If one neglects in Eq. (7), the changes in the electron temperature, i.e., $T_e=T$, we get for the output of the current component with frequency $2\omega_1-\omega_2$ using Eqs. (5) and (6) in the following form:

$$J_0(2\omega_1-\omega_2)=-NeV(2\omega_1-\omega_2) =-\tfrac{1}{2}n[Ne^4E_1^2E_2/ m^2kT\omega_1\omega_2(2\omega_1-\omega_2)(\omega_1\tau_0)], \quad (8)$$

where $\omega_1\tau_0\gg1$ and N is the carrier concentration. In Ref. 1, for $T_e=T$ there is no contribution to $J(2\omega_1-\omega_2)$. We shall now establish that the first term in Eq. (7) which leads to Eq. (8) is larger in its contribution to the current component $J(2\omega_1-\omega_2)$ than the other two terms. Using Eqs. (1)–(4), the temperature components are expressed by

$$T_e(2\omega_1)=-[e^2E_1^2\tau_0/3(1+\omega_1^2\tau_0^2)^2\omega_1mk] \times[2\omega_1\tau_0+i(1-\omega_1^2\tau_0^2)] \quad (9)$$

and

$$T_e(\omega_1-\omega_2) =-4e^2E_1E_2^*/3km(1+\omega_1^2\tau_0^2)(1+\omega_2^2\tau_0^2)(\omega_1-\omega_2) \times[\tau_0(\omega_1-\omega_2)-i(1+\omega_1\omega_2\tau_0^2)]. \quad (10)$$

It should be noted that Eqs. (9) and (10) differ from Eqs. (7a) and (7b) of Ref. 1, due to the inclusion of the drift term in Eq. (2). Combining Eqs. (5)–(7), (9), and (10), we write

$$J(2\omega_1-\omega_2)=\tfrac{1}{2}n\frac{Ne^4E_1^2E_2}{m^2kT\omega_1\omega_2(2\omega_1-\omega_2)} \times\left[-\frac{1}{\omega_1\tau_0}+i\frac{A}{(\omega_1\tau_0)^2}\right] =J_0(2\omega_1-\omega_2)[1-i(A/\omega_1\tau_0)], \quad (11)$$

where

$$A=\frac{6\omega_1^3-5\omega_2^3-30\omega_1^2\omega_2+25\omega_1\omega_2^2}{3(\omega_1-\omega_2)(2\omega_1-\omega_2)\omega_2}.$$

We have assumed $\omega\tau_0\gg1$ and retained terms up to $1/(\omega\tau_0)^2$. The first and the second term in the square bracket of Eq. (11) arise due to the electron drift and the changes in the electron temperature, respectively. It therefore follows that the contribution to the nonlinearity due to the drift term may be important when $(A/\omega_1\tau_0)\ll1$.

PHYSICAL REVIEW VOLUME 181, NUMBER 3 15 MAY 1969

Optical Spectra of Donor Impurities in InSb in High Magnetic Fields

R. KAPLAN
Naval Research Laboratory, Washington, D. C. 20390
(Received 16 December 1968)

Experimental studies of the donor-impurity excitation spectra in InSb in high magnetic fields have yielded good qualitative agreement with theoretical predictions with regard to transition energies, selection rules, polarization, and absorption constants. Quantitatively, the data demonstrate the need for including the effects of nonparabolicity in the theory, and indicate that corrections to the calculated ground-state energy are required. The usefulness of optical experiments in studying carrier freeze-out effects is briefly discussed.

I. INTRODUCTION

THE effects of a magnetic field on the energy levels and excitation spectra of impurity atoms in semiconductors are usually considered in the limiting cases of very small and very large magnetic fields. In the former case the effects appear as small shifts and splittings of the zero-field levels and optical transitions, while in the latter case there is a drastic qualitative change in the level structure and the excitation spectra. A number of theoretical calculations[1–4] for the high-field case have succeeded in giving a detailed account of the impurity states and optical transitions for donor

[1] Y. Yafet, R. W. Keyes, and E. N. Adams, J. Phys. Chem. Solids **1**, 137 (1956).
[2] R. F. Wallis and H. J. Bowlden, J. Phys. Chem. Solids **7**, 78 (1958).
[3] H. Hasegawa and R. E. Howard, J. Phys. Chem. Solids **21**, 179 (1961).
[4] H. Hasegawa, in *Physics of Solids in Intense Magnetic Fields*, edited by E. D. Haidemenakis (Plenum Press, Inc., New York, 1969).

impurities in a host semiconductor possessing an idealized band structure. A recent calculation[5] for donor impurities in InSb included conduction-band nonparabolicity and showed that this should lead to observable discrepancies between the earlier theories and experiment. In spite of the theoretical interest in the problem, there have been relatively few experimental studies of the high-field impurity excitation spectra. This is due largely to the difficulty in obtaining suitable semiconductors with sufficient purity, the need for very strong magnetic fields, and the fact that some of the optical transitions lie in the submillimeter and millimeter spectral regions. The most complete observations[6] of high-field impurity excitations to date have been made on donor impurities in InSb. These observations have been in general qualitative agreement with the theory.

The present paper describes the results of high-field experiments on donor impurities in InSb that were planned as a detailed quantitative test of the existing theories. The experiments have demonstrated the necessity of including real crystal effects, such as nonparabolicity, in the calculations. Furthermore, they indicate that additional refinements, such as the inclusion of central-cell corrections for the impurity ground state, may be required.

As far as possible in the present work, the impurity atoms have been treated as independent entities, which do not interact among themselves. In fact, strong magnetic fields are required to remove the interactions between neighboring impurities, producing the well-known "magnetic freeze-out." In order to minimize effects due to impurity interactions, the purest available materials have been used, and the experiments have been extended into the magnetic-field regime where carrier freeze-out is very nearly complete. Sample temperatures low enough to avoid thermal populating of low-lying excited states have been used. Effects due to carrier freeze-out have been taken into account where necessary in the analysis of the data.

The paper is organized as follows: Section II contains a brief description of several different theoretical approaches to the calculation of high-field impurity energy levels, wave functions, and optical spectra. In Sec. III, the experimental methods used in the present work are described. The data and their analysis appear in Sec. IV, and the conclusions in Sec. V.

II. THEORETICAL BACKGROUND

A. General Formulation

The problem of calculating the high-field impurity states has in all cases been approached within the framework of the effective-mass approximation. The hydrogenic effective-mass equation for charge carriers of effective mass m^*, in a semiconductor with dielectric constant κ containing impurities whose effective charge is the electronic charge $|e|$, in the presence of a magnetic field $\mathbf{H}$ directed along the z axis, may be written

$$\left(\frac{p^2}{2m^*}+\frac{\omega_c}{2}(xp_y-yp_x)+\frac{m^*\omega_c^2}{8}(x^2+y^2)-\frac{e^2}{\kappa r}\right)\times F(\vec{r})=EF(\vec{r}). \quad (1)$$

The quantity ω_c is the angular cyclotron frequency; $\omega_c=eH/m^*c$. For the present, the interaction between the spin magnetic moment of the charge carrier and the magnetic field is neglected, since its effect is assumed to be a shift of all the calculated energies by a uniform amount. Equation (1) may be rewritten in dimensionless form, in cylindrical coordinates, as

$$(-\nabla^2-i\gamma\partial/\partial\varphi+\tfrac{1}{4}\gamma^2\rho^2-2(\rho^2+z^2)^{-1/2})F(\rho,\varphi,z)=EF(\rho,\varphi,z). \quad (2)$$

In this formulation, energy is measured in units of the effective Rydberg Ry*, length in units of the effective Bohr radius a_0^*, and magnetic field in terms of the parameter γ. These quantities have the following definitions:

$$\mathrm{Ry}^*=m^*e^4/2\hbar^2\kappa^2, \quad (3)$$

$$a_0^*=\kappa\hbar^2/m^*e^2, \quad (4)$$

$$\gamma=\hbar\omega_c/2\ \mathrm{Ry}^*. \quad (5)$$

The field parameter γ may also be written as $\gamma=(a_0^*/\lambda_0)^2$, where λ_0, the cyclotron orbit radius, is given by $\lambda_0=(\hbar c/eH)^{1/2}$.

Equation (2) was first investigated in the high-field regime by Yafet, Keyes, and Adams[1] (YKA), who showed that, in the limit $\gamma\to\infty$, exact solutions can be written

$$F_{NMn}=\Phi_{NM}(\rho,\varphi)f_{NMn}(z). \quad (6)$$

The functions $\Phi_{NM}(\rho,\varphi)$ are the transverse part of the usual free-carrier solutions in a magnetic field in the absence of the Coulomb interaction, while the $f_{NMn}(z)$ satisfy a one-dimensional Schrödinger equation with an averaged Coulomb potential. The energies corresponding to the $\gamma\to\infty$ wave functions, Eq. (6), are

$$E_{NMn}=\hbar\omega_c(N+\tfrac{1}{2})+\epsilon_{NMn}. \quad (7)$$

For the bound impurity states, the ϵ_{NMn} assume discrete negative values whose magnitudes are small compared to $\hbar\omega_c$. Thus, in general appearance, the energy level spectrum in the high-field limit, neglecting spin, resembles a free-carrier Landau ladder with a set of discrete levels just beneath each rung of the ladder.

The formulation described above applies to the case of impurity states associated with a parabolic, spherical, nondegenerate band whose extremum is located at $k=0$.

[5] D. M. Larsen, J. Phys. Chem. Solids **29**, 271 (1968).
[6] R. Kaplan, J. Phys. Soc. Japan Suppl. **21**, 249 (1966).

These requirements are largely satisfied by donor impurities in InSb, aside from the spin degeneracy. The major discrepancies between the theoretical model and the experimental situation for InSb involve the strong nonparabolicity of the conduction band, and the possible inadequacy of the effective-mass approximation in describing the impurity ground state. These discrepancies were recently pointed out and considered by Larsen.[5]

For comparison with the experimental excitation spectra, theoretical results are required for the ground state and the excited states taking part in the optical transitions. The results of several calculations of the required quantities will now be summarized.

B. Calculations for Parabolic Conduction Band

Equation (2) is not separable at large but finite values of γ. Thus some approximate method of solution must be used. YKA obtained a lower bound to the ground-state binding energy by means of a variational calculation, using as a trial function a product function having the general form of Eq. (6). This method was extended to the calculation of the excited states and the optical spectra by Wallis and Bowlden[2] (WB), who used trial functions containing an additional factor $P_\lambda(z)$. The orthogonal polynomials $P_\lambda(z)$ alter the z dependence of the impurity wave functions for the excited states. In order to simplify the calculations, WB neglected a variational parameter, used by YKA, which affects the motion of the charge carriers in the plane transverse to the magnetic field. This is equivalent to assuming that the transverse motion is unaffected by the impurity potential, and results in a slight additional underestimation of the impurity binding energies, especially at lower fields.

In the notation used by WB, impurity states are identified by the quantum number set $(lm\lambda)$, where l is a positive integer or zero, and m is the quantum number for orbital angular momentum about the magnetic field and may take any integral value. In terms of these quantities, the quantum numbers used by YKA and others have the values

$$N=l+\tfrac{1}{2}(m+|m|), \quad M=m.$$

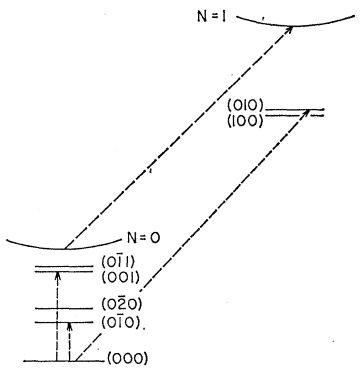

FIG. 1. Energy levels for a fixed value of the magnetic field, $\lambda>1$. The two lowest Landau levels are shown as curved lines, the discrete impurity states as flat lines. Free-carrier cyclotron resonance and three transitions from the ground state are indicated by the arrows.

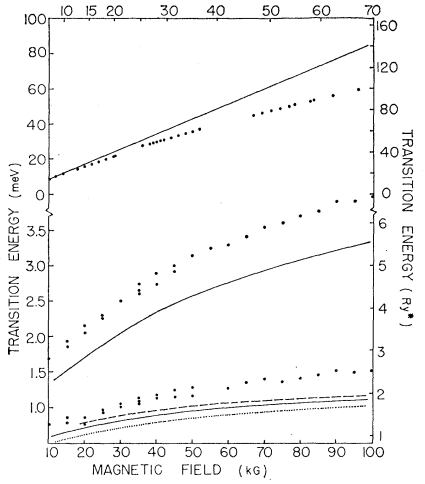

FIG. 2. Field dependence of the energies of the three predominant impurity transitions. The observed energies are indicated by the black circles. The curves show the following theoretical results: solid lines, Wallis and Bowlden (Ref. 2); dotted line, Hasegawa and Howard (Ref. 3); dashed line, Larsen (Ref. 5) (nonparabolic calculation). Note change in energy scale for the (000) → (010) transition.

From calculations of the matrix elements for electric dipole transitions between the ground and various excited states, WB concluded that three transitions predominate greatly over all others. (Strongly allowed transitions from excited initial states are assumed to be excluded by resorting to sufficiently low sample temperatures.) Each of these three transitions requires a different polarization of the electromagnetic radiation with respect to the magnetic field, as follows:

(000) → (0$\bar{1}$0), right circular polarization (RCP);
(000) → (001), $\mathbf{E}\|\mathbf{H}$;
(000) → (010), left circular polarization (LCP).

The second of these requires light propagating at an angle to the magnetic field $\mathbf{H}$, in order to provide a component of the electric vector $\mathbf{E}$ of the radiation along $\mathbf{H}$. In Fig. 1 the four states involved in these transitions are shown for a fixed value of the magnetic field, together with the free-carrier Landau levels. Several other bound states are also included. In the parabolic approximation, the binding energies of the (0$\bar{1}$0) and (010) states are equal. The calculated transition energies versus field for the three predominant impurity transitions at low temperature are shown by the solid lines in Fig. 2. All of these results are for the lower-energy spin state, in which the spin vector is parallel to the magnetic field (spin up, indicated ↑). Similar results obtain for the opposite spin state, but are not of concern here since the (000; ↓) state is not

populated at the temperatures used in the present work, and the transitions studied conserve spin.

According to WB the absorption coefficients $k(\omega)$ for the impurity transitions are given by

$$k(\omega)=\frac{8\pi^2 N_i|Q|^2}{hc\kappa^{1/2}}\left(\frac{\omega_0\Delta\omega}{(\omega-\omega_0)^2+(\Delta\omega)^2}\right), \quad (8)$$

where N_i is the concentration of electrons occupying the impurity ground state. For a particular transition, Q is the electric dipole matrix element, ω_0 is the angular resonant frequency, and $\Delta\omega$ is the half-width at half-maximum absorption. For the evaluation of peak absorption coefficients, Eq. (8) may be written

$$k(\omega_0)=\frac{8\pi^2 N_i|Q|^2}{hc\kappa^{1/2}}\frac{\omega_0}{\Delta\omega}. \quad (9)$$

The magnitudes of $k(\omega_0)$ for the various transitions are determined in great measure by $|Q|^2$. Expressions for $|Q|^2$ have been calculated by Wallis and Bowlden.[7] Equation (9) will be used later in comparisons between theoretical and experimental determinations of the absorption coefficients.

Trial functions having the form of Eq. (6) become progressively more unrealistic as γ decreases toward unity. In order to extend the usefulness of the variational calculations to low fields, Larsen[5] recalculated the ground and $M=\pm1$ excited states, using trial functions that resemble atomic hydrogen functions as $\gamma\to0$. The resulting impurity binding energies were somewhat higher than those obtained by WB, but the $M=0$ excited state (001) was not considered.

Hasegawa and Howard[3] (HH) applied the quantum-defect method to the solution of the one-dimensional Schrödinger equation for the Coulomb states $f_{NMn}(z)$. Their calculation yielded substantially higher binding energies for the ground and $M=\pm1$ excited states than any of the variational calculations. It was also shown by HH that as $\gamma\to\infty$ the oscillator strength for the (000) $\to$ (010) transition approaches unity, while those for all other transitions vanish.

C. Nonparabolicity and Central-Cell Corrections

The nonparabolicity of the InSb conduction band is manifested in a considerable increase of electron effective mass with increasing energy in the band. Since the effective Rydberg is proportional to m^*, the nonparabolicity should affect the energies of the impurity states, particularly those associated with higher Landau or spin levels. Impurity states associated with such levels would be expected to have larger binding energies.

Larsen's calculation[5] for the nonparabolic case shows that the binding energies of all the impurity states increase more rapidly with field than predicted by the earlier theories. The effect is most marked for the relatively high-lying $M=1$ excited state (010). It follows that the binding energies of the (0$\bar{1}$0) and (010) states are no longer equal. A further complication suggested by Larsen is the probable need for central-cell corrections to the ground state. These different effects can be studied independently by an appropriate series of experiments, as will be shown below.

III. EXPERIMENTAL METHODS

In order to observe the high-field donor-impurity transitions in InSb, transmission and photoconductivity measurements have been performed at wavelengths between about 15 μ and 3 mm, in magnetic fields up to 100 kG. A grating spectrometer with focusing optics was used at the shorter wavelengths out to about 50 μ. In the range 30 μ–3 mm, a Fourier transform spectrometer adapted[8] for light pipe operation was employed. Magnetic fields were provided either by superconducting solenoids or the Bitter-type solenoids of the Naval Research Laboratory high-field magnet facility. Samples could be mounted either in the Faraday geometry (propagation along the field direction), or Voigt geometry (propagation normal to the field). In the latter case, wire grid polarizers were sometimes used to obtain radiation polarized along or normal to the magnetic field. No attempt was made to produce circularly polarized radiation. At wavelengths between 15 and 120 μ, liquid-helium-cooled germanium photoconductive detectors doped with zinc, copper, beryllium, or gallium provided both high sensitivity and convenience for light pipe operation. At longer wavelengths, InSb free-electron bolometers were employed.

Sample temperatures were measured with a calibrated germanium thermometer buried in the sample mounting block. Temperatures between 1.5 and 4.2°K were obtained by pumping over the liquid helium used as coolant. Temperatures as high as about 80°K could easily be maintained by passing a current through a heater coil wound on the sample block. Actual cooling of the sample was accomplished by means of a helium exchange gas system. Proper choice of the exchange gas pressure facilitated the maintaining of desired sample temperatures.

The criterion used in the choice of InSb samples was high electrical mobility at 80°K. Samples generally had an excess donor concentration N_D-N_A of about 7×10^{13} cm^{-3}, and a mobility at 80°K of about 7×10^5 cm^2 (V sec)$^{-1}$. Slices cut from single-crystal ingots were ground and polished to the desired thickness. Thin samples were mounted on high-purity silicon substrates. For photoconductivity measurements, small areas were etched with CP_4, and pure indium was used to solder leads to these areas. Since at the beginning of the study no dependence of the measured quantities

[7] R. F. Wallis and H. J. Bowlden (unpublished results).

[8] R. Kaplan, Appl. Opt. 6, 685 (1967).

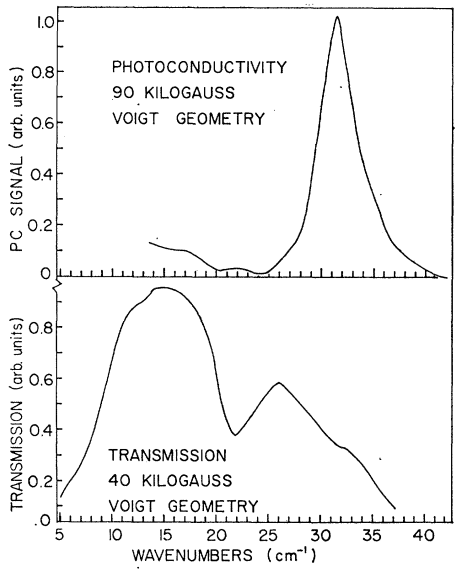

FIG. 3. Typical spectra obtained for the (000) → (001) transition, uncorrected for instrumental spectral response. Top, photoconductive response at 90 kG. Bottom, transmission observed at 40 kG using an InSb free-electron bolometer. The slow increase of energy with magnetic field for this transition is evident from the two spectra.

on crystal orientation was observed, subsequent work was done on unoriented single crystal samples.

Earlier work[6,8] had shown that the spectral dependence of the photoconductivity matched that of the absorption constant for the impurity and cyclotron resonance transitions. Photoconductivity spectra have proved more convenient and reliable than transmission spectra for determining such quantities as ω_0 and $\Delta\omega$. This is primarily because the resonant photoconductivity is a null-background technique. In eliminating the need for a detector, this technique also greatly simplifies the obtaining of data over a wide spectral range. However, for measurements of absorption constants, transmission spectra were required. Typical spectra obtained in the Voigt geometry for the (000) → (001) transition are shown in Fig. 3, uncorrected for spectrometer and detector response.

In addition to the three impurity transitions illustrated in Fig. 1, several other optical transitions have been studied in the present work. Free-carrier cyclotron resonance, also indicated in Fig. 1, always occurs at an energy slightly smaller than that of the (000) → (010) transition. This results in a doublet absorption[9] whose component intensities depend on the populations of the (000) impurity ground state and $N=0$ Landau level, and thus vary with temperature and magnetic field. The energy separation Δ of the doublet components is given by

$$\Delta=[E(010)-E(000)]-[E(N=1)-E(N=0)]. \quad (10)$$

Combined resonance transitions have also been studied; these occur at the energies $E(N=1;\downarrow)-E(N=0;\uparrow)$ for free carriers, and $E(010;\downarrow)-E(000;\uparrow)$ for localized electrons where the arrows indicate spin orientation. A doublet absorption is thus also observed in combined resonance, but its splitting may be expected[10] to differ from Δ.

IV. EXPERIMENTAL RESULTS AND ANALYSIS

A. Transition Energies

The observed impurity transition energies are plotted versus magnetic field in Fig. 2. Results obtained from both transmission and photoconductivity spectra are included. Theoretical values deduced from the impurity state energies calculated by WB are shown as solid lines. The (000) → (01$\bar{0}$) transition energies obtained by HH and Larsen are also included. As mentioned previously, the only theory which yields numerical results for the (000) → (001) transition is that of WB. In the case of the parabolic band calculations, the dimensionless results are plotted by assuming an effective mass $m^*=0.0138\ m_0$. This yields the relation $\gamma=0.7H$, with H measured in kG, and Ry*$=0.6$ meV for $\kappa=17$. In the case of the nonparabolic band calculation, the theoretical results assume bottom-of-the-band values $m^*=0.0138m_0$ and Ry*$=0.6$ meV. The nonparabolic band results were given directly in meV and kG by Larsen.

Since the (010) state is associated with the $N=1$, or second Landau level, the (000) → 010) transition energy is strongly affected by nonparabolicity in two ways. First, the (010) binding energy depends on the effective mass that is characteristic of the $N=1$ Landau level, which increases rapidly with magnetic field. Second, the $N=1$ Landau level energy increases less than linearly with field. The latter effect is responsible for most of the discrepancy between theory and experiment for this transition that appears in Fig. 2. To study the (010) binding energy directly, it is convenient to compare measured and calculated values of Δ, as shown in Fig. 4. Also plotted in this figure is the observed transition energy for (000) → (01$\bar{0}$), which for convenience will be denoted by δ. Typical spectra used in the determination of Δ and δ are shown in Fig. 5.

Figures 2 and 4 demonstrate only a general qualitative agreement between experiment and theory regarding the magnitudes and field dependence of the impurity transition energies. Certain of the discrepancies show the need for taking the conduction-band nonparabolicity into account in the theory. The nonlinear field dependence of the (000) → (010) energy demonstrates this need. However, the most direct evidence is provided by the observed divergence of the quantities δ and Δ as the magnetic field is increased.

[9] W. S. Boyle and A. D. Brailsford, Phys. Rev. **107**, 903 (1957).

[10] B. D. McCombe and R. Kaplan, Phys. Rev. Letters **21**, 756 (1968).

With the help of Eq. (10) and the definition of δ, the following relationship is easily deduced:

$$\delta-\Delta=[E(N=1)-E(010)]-[E(N=0)-E(0\bar{1}0)]. \quad (11)$$

The quantities in square brackets are the binding energies of the (010) and $(0\bar{1}0)$ states. These are equal in the parabolic approximation. However, as pointed out earlier, the $N=1$ Landau level is characterized by a larger value of m^* than the $N=0$ level. Thus the binding energy of (010) exceeds that of $(0\bar{1}0)$, and $(\delta-\Delta)>0$. This analysis is not affected by ground-state corrections, since the ground-state energy does not appear in Eq. (11). The experimental field dependence of $\delta-\Delta$ has been estimated from Fig. 4, and compared with Larsen's calculation for the difference in the binding energies of (010) and $(0\bar{1}0)$. This comparison yields agreement to within a few percent over the field range 20–100 kG, indicating that the effects of nonparabolicity have been correctly taken into account in the theory.

The inclusion of nonparabolicity in the theory strengthens the calculated field dependence of the impurity state binding energies, since the effective mass increases with field. However, this does not lead to an appreciable increase in the calculated (000) $\rightarrow$ $(0\bar{1}0)$ transition energy, which remains smaller than the observed value. Furthermore, the predicted field dependence of Δ now differs more strongly from the observed, reaching a peak and then decreasing at high fields. This behavior results from the fact that due to nonparabolicity, the calculated binding energy of (010) increases more quickly with field than that of (000), and eventually exceeds the latter. These disagreements with experiment may be accounted for by postulating[5] the need for central-cell corrections in the effective-mass theory. Such corrections would increase the ground-state energy, without materially affecting the excited states, since the latter distribute charge away from the impurity centers. The result would be an increase in all the impurity excitation energies, and an increase in Δ. Since the ground-state charge density at the impurity sites increases with magnetic field, all of these corrections should become progressively more important at higher fields. All of these features are in the right direction to improve the agreement with experiment.

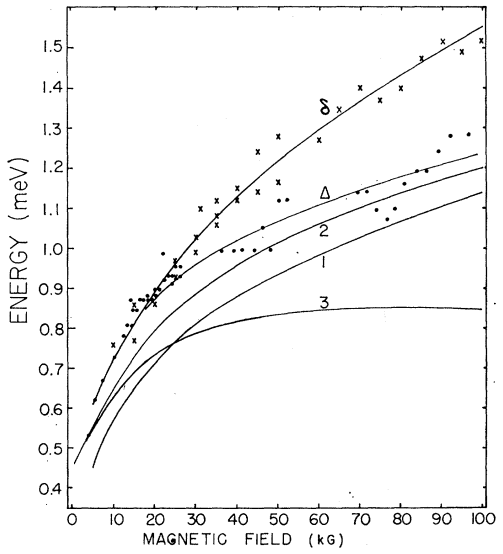

FIG. 4. Magnetic-field dependence of Δ, defined by Eq. (10), and δ, the (000) $\rightarrow$ $(0\bar{1}0)$ transition energy. Smooth curves have been drawn through the experimental points. The theoretical curves for Δ are identified as follows: 1, Wallis-Bowlden (Ref. 2); 2, Larsen (Ref. 5) (parabolic calculation); 3, Larsen (Ref. 5) (nonparabolic calculation).

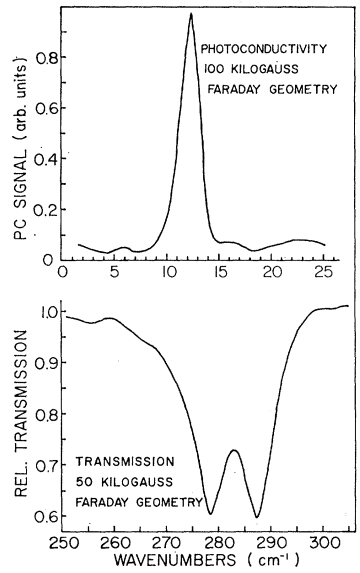

FIG. 5. Typical spectra used in determining the field dependence of the quantities δ and Δ. Top, the photoconductive signal at 1.5°K and 100 kG due to the (000) $\rightarrow$ $(0\bar{1}0)$ transition. Bottom, the doublet absorption due to free-carrier cyclotron resonance and the (000) $\rightarrow$ (010) impurity transition, at 50 kG. A Be-doped Ge photoconductive detector was used in this spectral region. To obtain relative transmission, runs were made at the desired field value and a value for which the resonances occurred in another spectral region, and their ratio taken. To obtain approximately equal doublet component intensities at this field, the sample temperature was rasied to 6.5°K.

The experimental spectra can be used to estimate the central-cell correction. Since the spectra do not yield the ground-state energy directly, the procedure followed would be to compare the observed and calculated transition energies, particularly for (000) $\rightarrow$ $(0\bar{1}0)$. The effects of nonparabolicity on this transition energy should be small, since the states involved lie close together fairly low in the band. Assuming that the calculated (000) and $(0\bar{1}0)$ energies are accurate within the effective-mass approximation, the difference in experimental and theoretical transition energies gives directly the central-cell correction to the ground state. In Fig. 6 the points show the results of subtracting the (000) $\rightarrow$ $(0\bar{1}0)$ transition energies calculated by

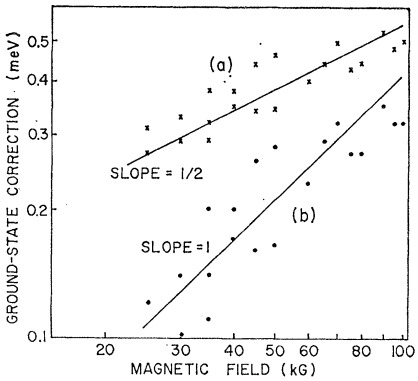

FIG. 6. Field dependence of the ground-state energy correction deduced from comparisons between theoretical and experimental transition energies for (000) → (0$\bar{1}$0). In (a) the energies calculated by Hasegawa and Howard (Ref. 3) have been subtracted from the data, while in (b) the theoretical nonparabolic results of Larsen (Ref. 5) have similarly been used. Straight lines of slope 0.5 and 1.0 appear to fit the results over the field range 25–100 kG, as shown.

HH and Larsen from each of the observed transition energies. The slopes of straight lines fitted to the points yield the power-law dependence of the ground-state correction on magnetic field. The correction varies approximately as $H^{1/2}$ if the theory of HH is assumed to give an accurate description of the (000) and (0$\bar{1}$0) levels within the effective-mass approximation. Similarly, the correction varies linearly with field for the Larsen calculation. Larsen has suggested[5] that an $H^{3/2}$ dependence would result from a simple model which assumes that the charge density at the impurity site varies as $(1/\lambda_0)^3$ since the cyclotron radius λ_0 varies as $H^{-1/2}$. However, almost all of the shrinkage of the charge distribution actually occurs in the directions transverse to the field. Thus a nearly linear field dependence of the central-cell correction might be expected from this simple model.

Considering the 10–15% difference between the ground-state binding energies calculated by HH and Larsen (see Fig. 8), it is not surprising that the two theories lead to widely differing ground-state corrections when compared with the optical excitation spectra. In the absence of further experimental or theoretical work, quantitative intrepretation of the results shown in Fig. 6 appears difficult. If these results do in fact imply a large central-cell correction, the observation of "chemical shifts" of the ground-state energies for different donor impurities in InSb might be possible. Such shifts, which would be strongest at high fields, should show up directly in measurements of the (000) → (0$\bar{1}$0) and (000) → (001) energies, and in measurements of Δ.

B. Polarization and Selection Rules

The polarization rules for the impurity transitions have been experimentally tested as far as possible with the techniques available. Absorption or photoconductivity due to the (000) → (001) transition appeared only in the Voigt geometry, in which approximately half of the incident radiation has the required polarization. A polarizer oriented to reflect all radiation with $\mathbf{E}\|\mathbf{H}$ destroyed the signal, thus verifying that the (000) → (001) transition requires radiation with $\mathbf{E}\|\mathbf{H}$. Similar experiments showed that the (000) → (0$\bar{1}$0) and (000) → (010) transitions require radiation with $\mathbf{E}\perp\mathbf{H}$. Since circularly polarized radiation was not used, it was not possible to discriminate against RCP- or LCP-allowed transitions separately.

The three impurity excitations discussed above are the only transitions from the ground state that have been observed in the present work. This result is consistent with the predictions of WB regarding transitions to bound excited states. Photoionization transitions from the ground state to the continuum levels have not been observed.

C. Absorption Constants

Absorption constants for the impurity excitations have been measured as a function of magnetic field. Comparison of the results with theoretical predictions is hampered, however, by the complexity of the experimental situation. The two major difficulties arise from the carrier freeze-out effect, which causes the ground-state population to vary with field, and electron-optical phonon interactions[11] which split and broaden the (000) → (010) absorption in fields between 25 and 50 kG.

The measurements employed several samples cut from the same small region of a single-crystal ingot having uniform impurity concentration and mobility. Different sample thicknesses were used to study the three impurity transitions, whose strengths differed considerably. In each case the sample thickness d was chosen to keep the product $k(\omega_0)d$ near unity. Sample thicknesses used were the following: for the (000) → (010) transition, 0.01 cm; for (000) → (001), 0.01 and 0.033 cm; and for (000) → (0$\bar{1}$0), 0.15 cm. The peak absorption coefficients were measured for a sample temperature of 4.8°K.

To obtain an estimate of the field dependence of the ground-state population at 4.8°K, the absorption coefficient for free-carrier cyclotron resonance was also measured. The sum of the four measured absorption coefficients at 25 kG was then assumed to be proportional to the field-independent total excess electron concentration $N_D - N_A$. This assumption, as well as others required in the analysis of the data, will be discussed below. Similarly, the field-dependent sum of the three impurity transition absorption coefficients was assumed proportional to the ground-state concentration. The ratio of these sums gives the fraction of excess electrons in the ground state. The absorption

[11] R. Kaplan and R. F. Wallis, Phys. Rev. Letters **20**, 1499 (1968).

coefficient data were then normalized by dividing the observed values of $k(\omega_0)$ by the fraction of excess electrons in the ground state. The result shown in Fig. 7, gives $k(\omega_0)$ versus H for the case in which the ground-state population is just N_D-N_A at all fields. In this figure the error bars indicate the uncertainty in the original measurements of $k(\omega_0)$, and do not include uncertainty due to the analysis.

The theoretical curves in Fig. 7 were calculated from Eq. (9). Hall measurements on the samples yielded $N_D-N_A=7\times10^{13}$ cm^{-3}, while the value $\Delta\omega=0.25$ meV was derived from the absorption and photoconductivity spectra. The dashed and solid curves were obtained by using for ω_0 the theoretical and experimental results, respectively. Use of the latter leads to an empirical correction to the theoretical results. However, the correction is only partial, since the theoretical matrix elements for the impurity transitions still partially determine the solid curves.

Agreement between theory and experiment in Fig. 7 is satisfactory, with regard to the gross differences in $k(\omega_0)$ among the impurity transitions. The experiments cannot very well be said to demonstrate the predicted field dependence of $k(\omega_0)$, although they are consistent with this feature of the theory. They also seem consistent with the corrections applied to the theory by using the experimentally determined transition energies. These corrections involve both nonparabolicity, which decreases the (000) → (010) absorption coefficient, and ground-state energy effects, which tend to increase all of the $k(\omega_0)$ values.

The assumptions required in the foregoing analysis may now be considered. First, it was assumed that the free-carrier cyclotron resonance and the three impurity transitions virtually exhaust the excess electron oscillator strength for the two initial states involved. This is expected theoretically for the case of a parabolic conduction band, and should be only very slightly changed for the case of InSb. Experimentally, the only other transitions found in the present work, aside from those induced by coupling with optical phonons, were free-carrier and impurity combined resonance. These two transitions, which owe their appearance to the conduction-band nonparabolicity, are at least two orders of magnitude weaker than cyclotron resonance at the fields used. Second, it was assumed that the excess electrons occupied either continuum states, or the impurity ground state. This was based on the observation that although the excited-state transitions $(0\bar{1}0) \rightarrow (0\bar{2}0)$ and $(0\bar{1}0) \rightarrow (0\bar{1}1)$ are strongly allowed, they were absent from the optical spectra. [This fact also shows that the $(0\bar{1}0) \rightarrow (100)$ transition was not responsible for a measurable part of the intensity attributed to free-carrier cyclotron resonance, which occurs at virtually the same energy.] The apparent presence of electrons both in continuum states and the impurity ground states, but not in excited states of intermediate energy, is not currently understood. The

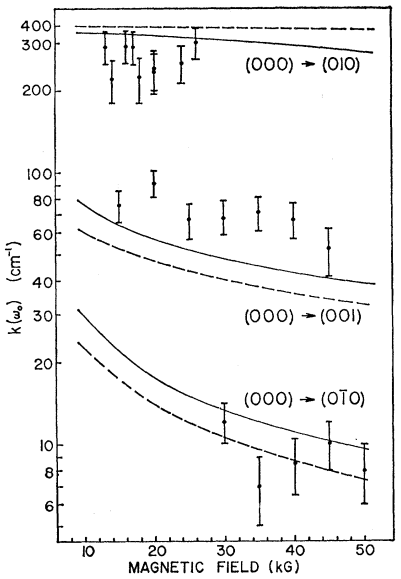

FIG. 7. Magnetic-field dependence of the peak absorption constants $k(\omega_0)$ for the three impurity transitions from the ground state. The results assume a ground-state concentration of $N_D-N_A=7\times10^{13}$ cm^{-3}. The dashed lines show the theoretical results of Wallis and Bowlden (Ref. 2) obtained from Eq. (9). The solid lines were obtained from the same equation by substituting experimentally determined values of ω_0. Error bars indicate the uncertainty in measurements of the absorption constants, but not in estimates of the ground-state concentration used to plot the data.

presence of free carriers at the field strengths used, even at very low temperatures, can be explained[12,13] on the basis of spatial fluctuations of the impurity potential, which introduce a tail in the continuum density of states. A third assumption made in the analysis was that the incident radiation was unpolarized. This applies to transitions requiring circularly polarized light, where it was assumed that half of the incident intensity had the correct polarization. In fact, the interferometer optics introduce some polarization of the radiation. The polarization is destroyed, however, during passage through the 1.9-cm-diam light pipe system. This was checked experimentally by observing cyclotron resonance in thick samples; the transmitted intensity at the transition energy was found to be just half that with the field removed. Finally, a fourth assumption was that the absorption linewidths were equal and constant under varying magnetic field. The widths of the (000) → $(0\bar{1}0)$ absorption lines appeared somewhat smaller than those of the other three transitions studied. All of the latter were consistent with the collision broadening expected for free-carrier cyclotron resonance in the InSb material used. A quantitative study of the broadening was not made. Variations in linewidth contribute to the experimental uncertainty in Fig. 7.

[12] A. L. Efros, D. L. Mitchell, and M. I. Dyakonov, Bull. Am. Phys. Soc. 13, 1433 (1968).
[13] M. I. Dyakonov, A. L. Efros, and D. L. Mitchell, Phys. Rev. 180, 813 (1969).

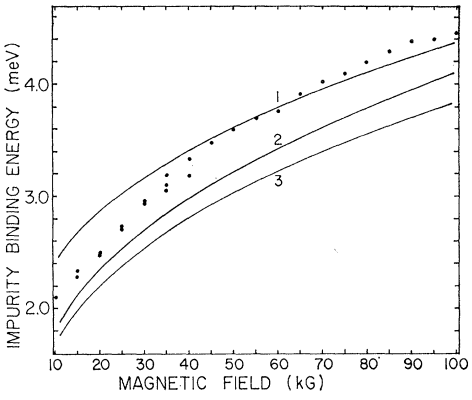

FIG. 8. Magnetic-field dependence of the impurity binding energy. The points were obtained by adding the theoretical (Ref. 2) (001) binding energy to the observed (000) → (001) transition energy at each field value. The curves represent the following calculations: 1, Hasegawa and Howard (Ref. 3); 2, Larsen (Ref. 5) (nonparabolic); 3, Wallis and Bowlden (Ref. 2).

In general, it appears that while the measured absorption coefficients are in good qualitative agreement with theory, an attempt at accurate quantitative measurement would encounter many difficulties.

D. Relation to Transport Measurements

Recently, there have been a number of theoretical and experimental studies of carrier freeze-out in InSb, based on the observation and analysis of charge transport in a magnetic field. One goal of these studies has been the determination of the donor-impurity ionization energy E_b. It is of interest to compare values of E_b obtained from transport measurements with the results of the optical-excitation studies. While the latter do not determine E_b directly, accurate values can be derived by adding to the observed (000) → (001) transition energy, the calculated (001) binding energy. The latter quantity is very nearly field-independent above 15 kG, and its value is affected only slightly by nonparabolicity and central-cell corrections. Furthermore, it contributes only about 10% of the magnitude of E_b at 50 kG, and less at higher fields. The field dependence of E_b determined by adding the (001) binding energy calculated by WB to the observed (000) → (001) optical excitation energy is shown in Fig. 8. For comparison, the results of several theoretical studies of the field dependence of E_b are included in the figure.

The results of the transport measurements have been contradictory. Analysis of the temperature and magnetic-field dependence of the Hall coefficient for samples similar to those described in Sec. III yielded[14] a donor-impurity binding energy considerably smaller than that deduced from the present optical measurements. Earlier transport work[15–17] on relatively pure samples gave similar results. It has been suggested[17,18] that the excitation energy observed in these experiments was, in fact, the (000) → (0$\bar{1}$0) energy, and that the (0$\bar{1}$0) levels can overlap to form an impurity band[5,18] even though the ground states are noninteracting. On the other hand, similar transport measurements[19,20] on samples with $N_D - N_A \approx 10^{15}$–$10^{16}$ cm^{-3} have yielded ground-state binding energies close to those deduced from the optical excitation spectra.

Analysis of the transport measurements may be complicated by a number of factors, among which are screening of the impurity potential, conduction in several bands, and inhomogeneous electric fields due to the free- and localized-electron distributions. For studies of carrier freeze-out, the optical-excitation experiments appear to avoid these difficulties, while providing the fractions of electrons in free and localized states. The electron distribution can readily be studied while varying the sample temperature, magnetic field, or other parameters of the experiment.

V. CONCLUSIONS

Experimental studies of the donor-impurity excitation spectra in InSb in strong magnetic fields show good qualitative agreement with theoretical predictions that are based on the effective-mass approximation and assume an idealized band structure. Quantitatively, however, the data demonstrate the need for including the effects of nonparabolicity in the theory, and are in agreement with a recent calculation for this effect. Furthermore, the data indicate that corrections to the calculated ground state are required, but an accurate estimate of the central-cell corrections could not readily be obtained by comparison with the theoretical results. This is because the latter show considerable diversity in estimating the hydrogenic effective-mass ground-state energy. Finally, the optical experiments appear to be useful for studies of magnetic-field–induced carrier freeze-out at low temperatures.

ACKNOWLEDGMENTS

Helpful discussions with Dr. R. F. Wallis, Dr. D. L. Mitchell, Dr. B. D. McCombe, and Dr. D. M. Larsen in the course of this work are gratefully acknowledged.

[14] H. Miyazawa and H. Ikoma, J. Phys. Soc. Japan **23**, 290 (1967).

[15] F. Ya. Nad' and A. Ya. Oleinikov, Fiz. Tverd. Tela **6**, 2064 (1964) [English transl.: Soviet Phys.—Solid State **6**, 1629 (1965)].

[16] E. H. Putley, in *Semiconductors and Semimetals*, edited by R. K. Willardson and A. C. Beer (Academic Press Inc., New York, 1966), Vol. 1.

[17] R. J. Sladek, J. Phys. Chem. Solids **5**, 157 (1958).

[18] J. Durkan and N. H. March, J. Phys. **C1**, 1118 (1968).

[19] O. Beckman, E. Hanamura, and L. J. Neuringer, Phys. Rev. Letters **18**, 773 (1967).

[20] L. J. Neuringer, in *Proceedings of the Ninth International Conference on Physics of Semiconductors, Moscow, 1968*, edited by S. M. Ryvkin (Nauka Publishing House, Leningrad, 1968).